LEVEL *C*

A SURFACE ACOUSTIC WAVE (SAW) PRESSURE SENSOR EVALUATION (U)

FINAL REPORT FOR THE PERIOD
March 27, 1979 through September 27, 1979

GENERAL ORDER NO. 41023
CONTRACT NO. N62269-79-C-0325

DOCUMENT NO. ERC41023.11FR

Prepared for

Naval Air Development Center
Warminster, PA 18974

DTIC
SELECTED
AUG 4 1980
C

E. J. Staples
Principal Investigator

MAY 1980

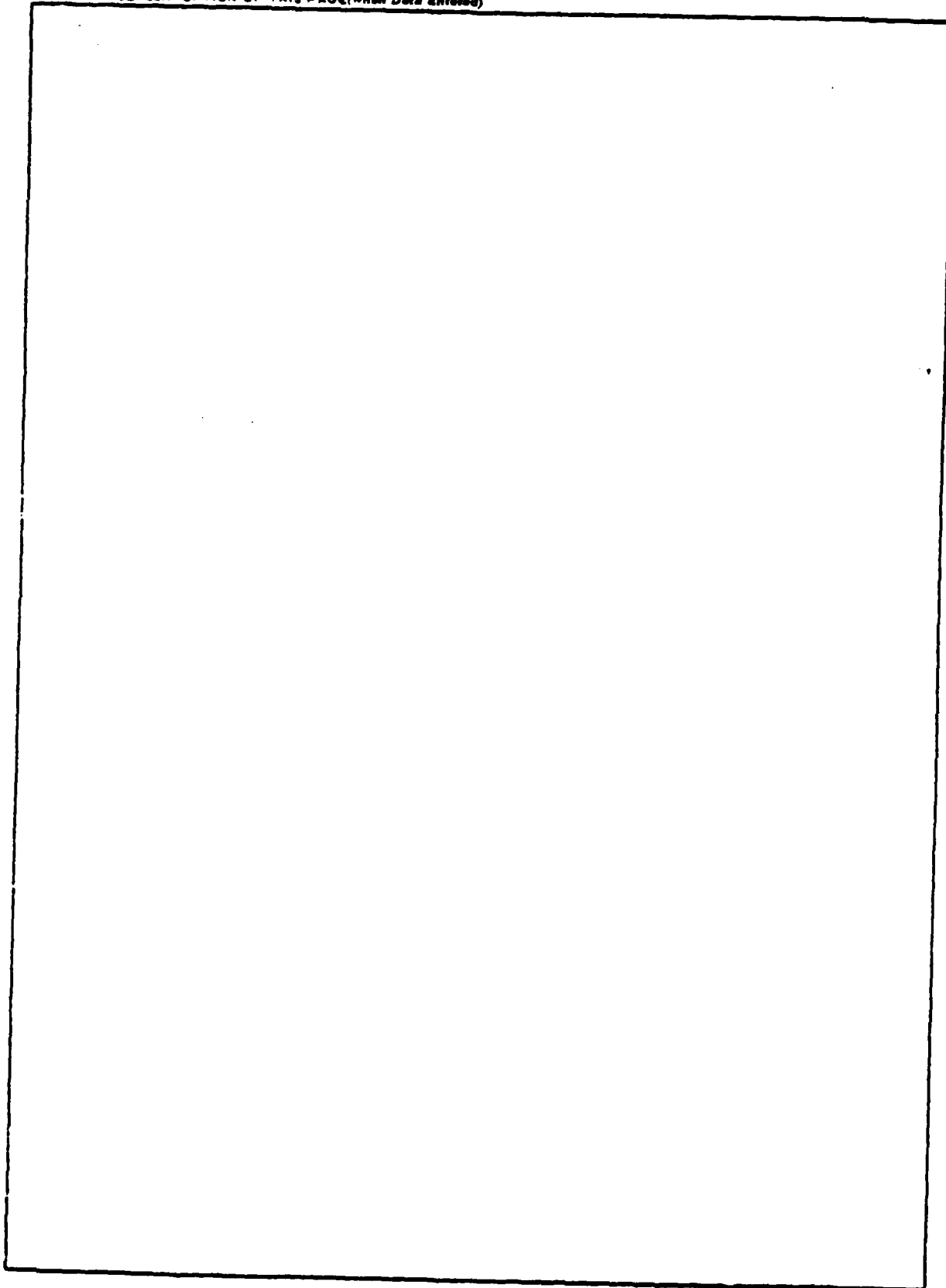Approved for public release; distribution unlimited

Rockwell International

SECURITY CLASSIFICATION OF THIS PAGE *(When Data Entered)*

(19) REPORT DOCUMENTATION PAGE	READ INSTRUCTIONS BEFORE COMPLETING FORM

1. REPORT NUMBER	2. GOVT ACCESSION NO.	3. RECIPIENT'S CATALOG NUMBER
NADC 79001-30	AD-A087 567	

4. TITLE *(and Subtitle)*	5. TYPE OF REPORT & PERIOD COVERED
A SURFACE ACOUSTIC WAVE (SAW) PRESSURE SENSOR EVALUATION	Final Report 3/27/79 through 9/27/79
	6. PERFORMING ORG. REPORT NUMBER ERC41023. /IFR

7. AUTHOR(s)	8. CONTRACT OR GRANT NUMBER(s)
E. J. Staples	N62269-79-C-0325

9. PERFORMING ORGANIZATION NAME AND ADDRESS	10. PROGRAM ELEMENT, PROJECT, TASK AREA & WORK UNIT NUMBERS
Electronics Research Center Rockwell International Corporation Thousand Oaks, CA 91360	(14) ERC41023.11FR

11. CONTROLLING OFFICE NAME AND ADDRESS	12. REPORT DATE
Receiving Officer Naval Air Development Center Warminster, PA 18974	May 80
	13. NUMBER OF PAGES 60

14. MONITORING AGENCY NAME & ADDRESS(*if different from Controlling Office*)	15. SECURITY CLASS. *(of this report)*
Final rept. 27 Mar - 27 Sep 79	UNCLASSIFIED
	15a. DECLASSIFICATION/DOWNGRADING SCHEDULE

16. DISTRIBUTION STATEMENT *(of this Report)*

Approved for public release; distribution unlimited

17. DISTRIBUTION STATEMENT *(of the abstract entered in Block 20, if different from Report)*

18. SUPPLEMENTARY NOTES

19. KEY WORDS *(Continue on reverse side if necessary and identify by block number)*

ASW sonobuoy hydrophone	Oscillator phase noise
Surface Acoustic Wave (SAW) sensor	Time domain frequency stability
SAW resonator/oscillator	FM deviation
SAW sensor system	Underwater sensitivity dB re 1V/uPa

20. ABSTRACT *(Continue on reverse side if necessary and identify by block number)*

The objective of this project was to evaluate the performance of surface acoustic wave (SAW) oscillators for potential application to SAW sonobuoys. The tests included the following: (1) oscillator frequency and time domain stability, (2) static loading sensitivity tests, and (3) underwater sensitivity and frequency response tests performed on a SAW hydrophone feasibility model. In summary, the results show that the SAW sensor is comparable in sensitivity to hydrophones currently available, typically -180 dB re 1V/uPa

DD FORM 1473

TABLE OF CONTENTS

1.0 SUMMARY

The objective of this project was to evaluate the preformance of surface acoustic wave (SAW) oscillators as underwater sensors for potential application to ASW sonobuoys. Described in this report are the results of performance tests on a feasibility model SAW sensor delivered to the Naval Air Development Center. The tests include the following: (1) oscillator frequency and time domain stability, (2) static loading sensitivity tests and (3) underwater sensitivity and frequency response tests performed on a prototype SAW hydrophone.

In summary, the results show that the SAW sensor is comparable in sensitivity to hydrophones currently available, typically -180 dB re 1 V/uPa. The SAW sensor may be useful for applications requiring remote seismic sensing and telemetry.

2.0 OBJECTIVES

The objective of this project was to design, fabricate and evaluate a feasibility model Surface Acoustic Wave (SAW) pressure sensor for potential application to ASW sonobuoys. Such a sensor has a theoretical capability to provide improved performance in a smaller volume and at a lower cost. This effort was to attempt to quantify key parameters of this device in order to determine its compatibility with current passive ASW sensors. In addition, this effort was to investigate the compatibility of this sensor with a multi-channel sonobuoy transmitter. The SAW sensor performance goals are as shown in Table I.

Table I

SAW Sensor Performance Goals

No-Load output frequency	:	125 kHz -0.015%
Temperature Range	:	+3 to +30°C
Sensitivity	:	-180 dB re 1 V/uPa
Directivity	:	Omnidirectional
Modulation	:	10 Hz to 10 kHz

2.1   Statement of Work

Three specific tasks were included in the statement of work:

2.1.1   Task 1

Design, fabricate, and deliver a feasibility model Surface Acoustic Wave pressure Sensor suitable for use in ASW sonobuoys.

2.1.2   Task 2

Investigate the performance of SAW sensors by measuring certain key parameters such as sensitivity, noise floor, and investigate their compatibility with multi-channel sonobuoy transmitters.

2.1.3   Task 3

Deliver to the Naval Air Development Center data in the form of monthly progress reports, a final technical report, part lists, and engineering drawings of the feasibility model.

3.0 TECHNICAL RESULTS

3.1 Saw Oscillators

During this project a total of 12 SAW oscillators were fabricated. Each oscillator consisted of a high Q SAW resonator and an RF amplifier. The SAW resonator provided a closed loop feedback path for the amplifier resulting in the build-up of stable oscillations at the resonant frequency of the crystal. Oscillator performance was determined primarily by the characteristics of the resonator; however the oscillator circuit design was also a factor effecting the overall stability.

3.1.1 SAW Resonators

3.1.1.1 Resonator Fabrication

Saw resonators[1] are fabricated by photolithographic techniques similar to transistors. Polished single crystal substrates, 0.020 x 0.55 inch diameter, were used for this project. A typical electrode pattern for a SAW resonator is depicted in Fig. 1, and consists of three regions: two electrode gratings on either side of an interdigital transducer (idt). The resonant frequency is primarily determined by the spacing between lines in the electrode pattern, hence the need for accurate size control during photographic reductions. During this project photomasks were made so as to replicate resonator patterns on quartz disks at 61 MHz and 61.125 MHz (0.0005 inch lines). The electrode material is aluminum which acoustically matches
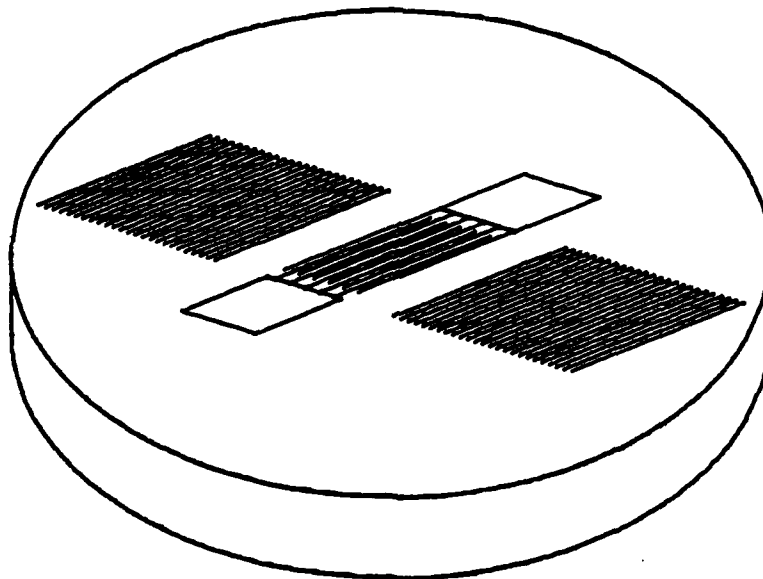
Fig. 1 Electrode pattern for typical SAW resonator.

quartz and can be easily etched into high resolution electrode patterns. After electrode delineation the quartz is etched between the lines of the gratings on either side of the idt. Etching the quartz results in high Q and also is used to place the resonator on its final frequency. The SAW resonator crystals are strong and can easily be handled provided care is taken not to scratch the soft aluminum electrode pattern on the polished side. Should the crystal require cleaning a mild dishwashing soap such as "Joy" applied with a foam covered cotton swab is recommeded. This is to be followed by a methanol rinse and blow dry. Electrical connection to the resonator is made by thermo-compression bonding 0.0015 inch gold wire to the bonding pads of the electrode pattern. An alternate method would be to attach wires by conductive epoxy.

3.1.1.2 Electrical Characteristics

Following fabrication, the electrical characteristics of the SAW resonators were measured using an HP8505 phase locked network analyzer. The basic equivalent circuit of resonator is shown in Fig. 2 and consists of a series resonant circuit, R1-C1-L1, shunted by the static capacitance of the electrode pattern plus any parasitic capacitances associated with external connectors. The static capacitance was typically 8 pf for the 61 MHz resonators. The Q of the resonator $Q = 2\pi f L_1 / R_1$, is a measure of the device selectivity and was determined by using a three-point measurement technique.[2] The voltage reflection coefficient, S11, of each SAW resonator was measured and plotted as shown in Fig. 3. Overlaying a Smith chart or transforming to the impedance plane provided the data for each crystal
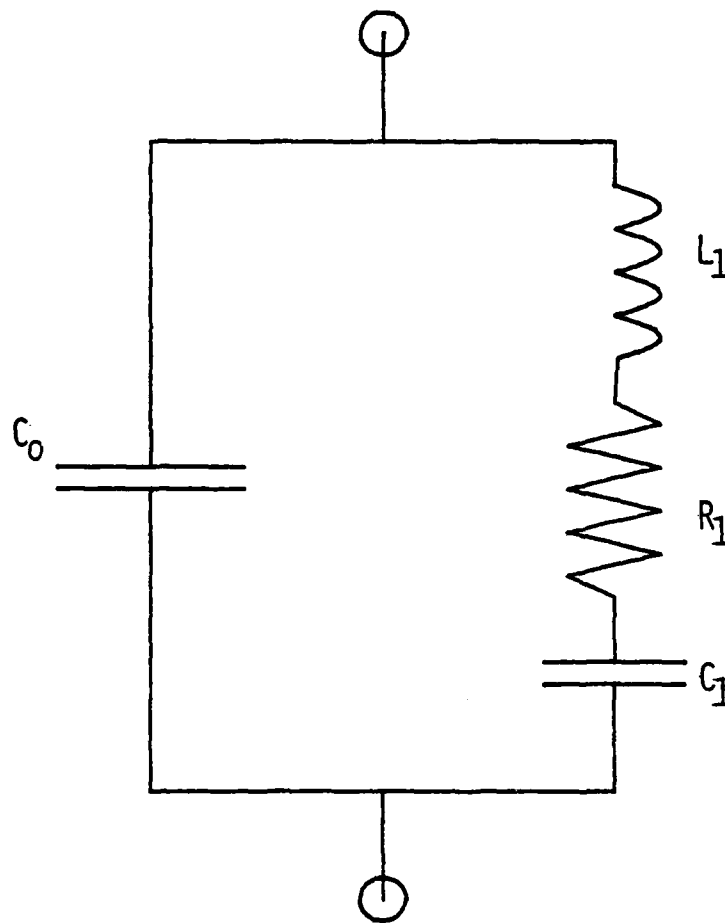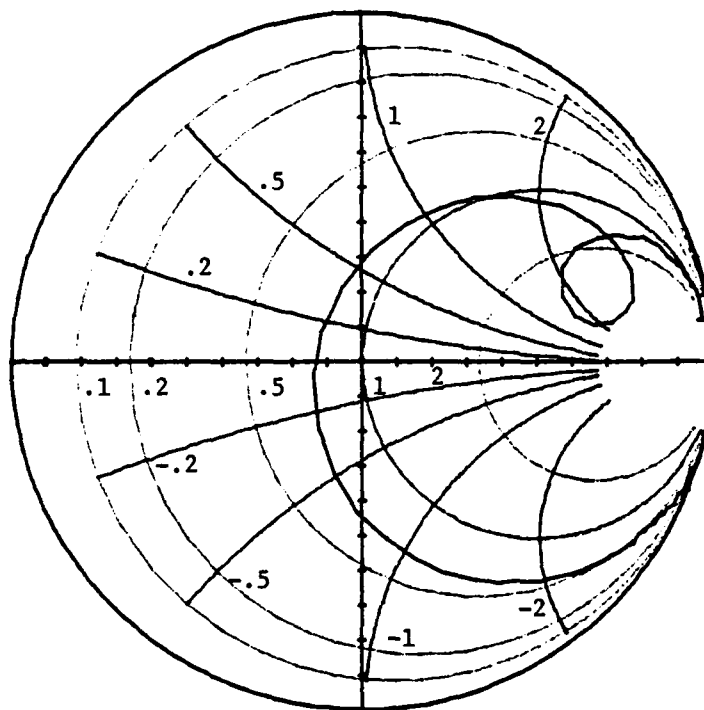
Fig. 2 SAW resonator lumped equivalent circuit.

Fig. 3 Experimental input voltage reflection coefficient,
S11, of a SAW resonator.

necessary to calculate the values of each element in the equivalent circuit of Fig. 2. Typical Q and resistance values for unsealed SAW resonators were >25,000 and <40 ohms respectively.

3.1.1.3 Temperature Stability

Surface acoustic wave resonator frequency as a function of temperature is determined by the substrate (quartz) expansion coefficients and elastic constants behavior with temperature. Since the substrate is anisotropic specific orientations provide better temperature stability than others. For surface acoustic wave devices, rotated Y-cuts of quartz provide the best stability and the frequency is a quadratic function of temperature about a turning point temperature, T_o. For this project a rotated y-cut of quartz was selected to provide a turning point of 25°C. Temperature stability was measured using an HP8505 phase locked network analyzer to track phase through the crystal while the temperature was varied. The measured turning point was typically 16°C as shown in Fig. 4. Also shown is a least squares fit to the data in the form of a polynominal: $\Delta F/F = P_o + P_1 + P_2 T^2$. Over a 50°C range the SAW resonator will deviate -20 ppm maximum.

3.1.2 Oscillators

During this project a total of 12 SAW oscillator circuits fabricated. Circuit design was either of the Pierce or Clapp type. For each type voltage sensitivity was measured as well as frequency and time domain stability.
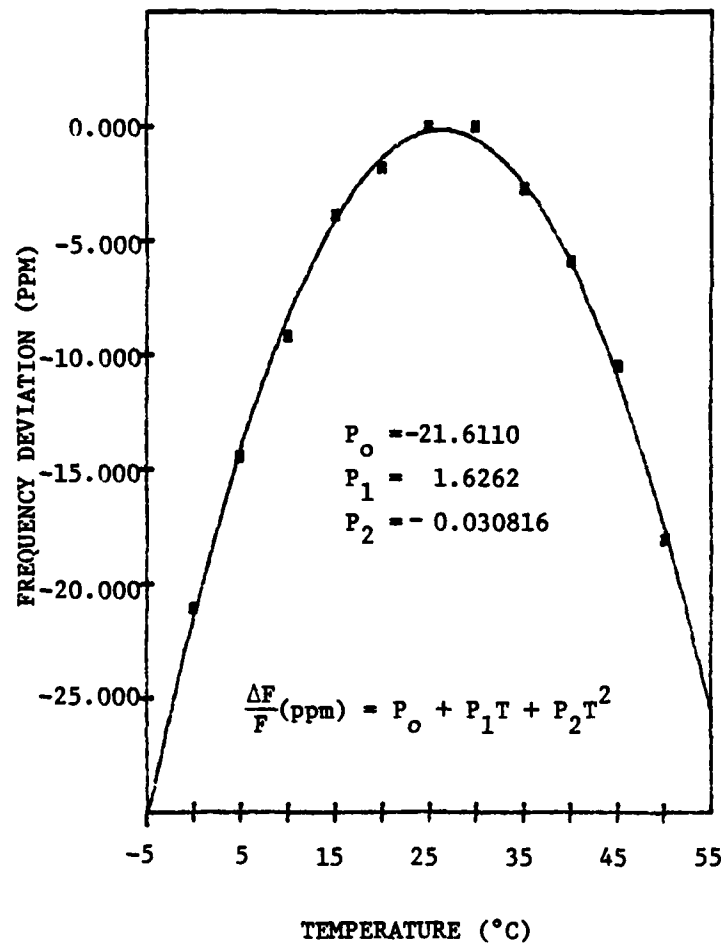
F-6-8-62B, Xtal #2

Fig. 4 Frequency vs temperature characteristic of SAW resonators.

3.1.2.1 Circuit Design

Early prototype oscillators were of the Pierce type and used diffused metal oxide (DMOS) transistors. Although this type of circuit provides excellent stability it was prone to not accepting crystals with widely different series resistances. Later designs utilized the Clapp circuit shown in Fig. 5. In this circuit the crystal resonance is with respect to system ground which makes crystal mounting and lead attachment simpler. All twelve of the final oscillators were of the Clapp type and were capable of accepting crystals with series resistances in the range 30-100 ohms. The circuit design itself is straightforward and follows well established techniques for feedback amplifier design.[3]

3.1.2.2 Stability

Instability in the SAW oscillators was found to result primarily from power supply variations and thermal changes coupled through the frequency-temperature characteristic of the SAW oscillator crystal. Power supply sensitivity is shown in Fig. 6 for both Pierce and Clapp oscillator circuits. The Clapp circuit was more nonlinear at high voltages and in this range the oscillator was less sensitivity to power supply variations.

Time and frequency domain stability were measured using a HP5390 Stability Analyzer. Time domain stability or Allan variance is shown in Fig. 7 for typical oscillator. The goal was to achieve a stability of 1×10^{-11} or better. Although this was not achieved, the stability shown in Fig. 7 is quite good considering the crystal was unpackaged and operating in
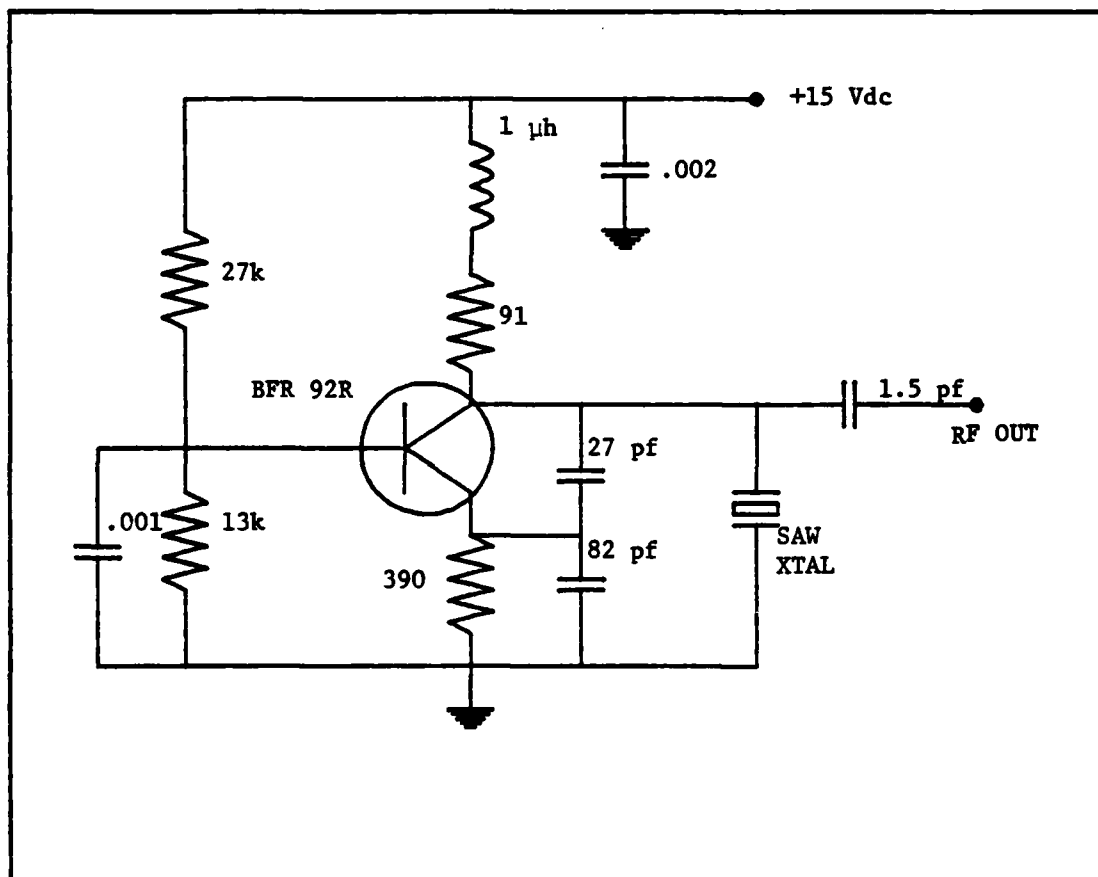
Fig. 5 Clapp oscillator circuit used with SAW resonator crystals.
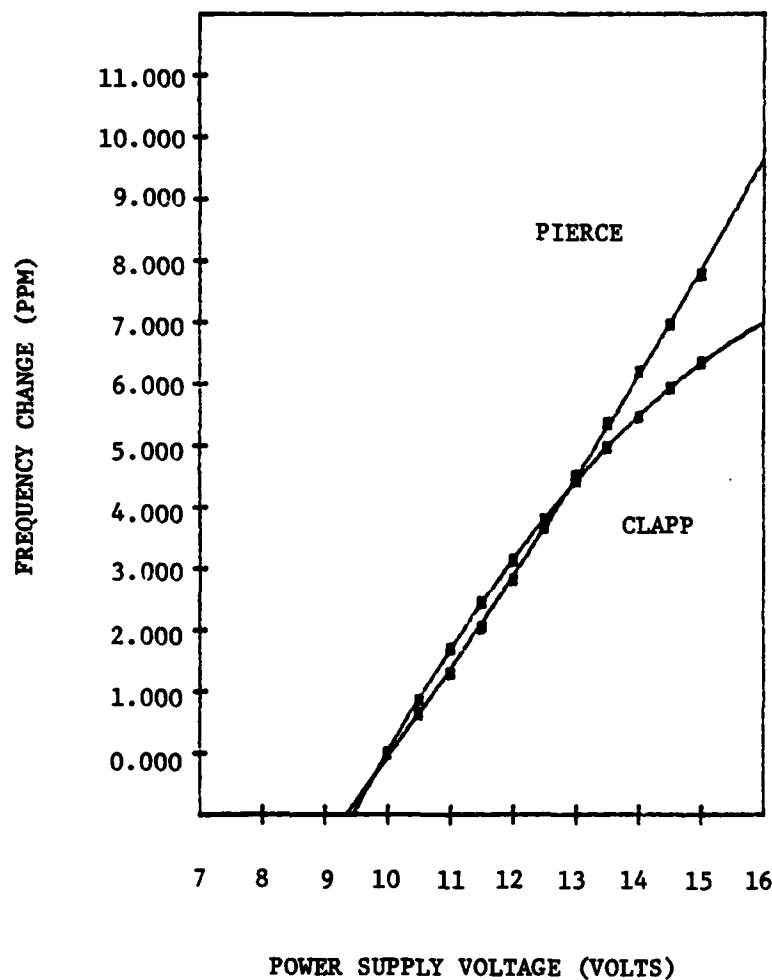
12

POWER SUPPLY SENSITIVITY

Fig. 6 Frequency vs power supply voltage for Pierce and Clapp
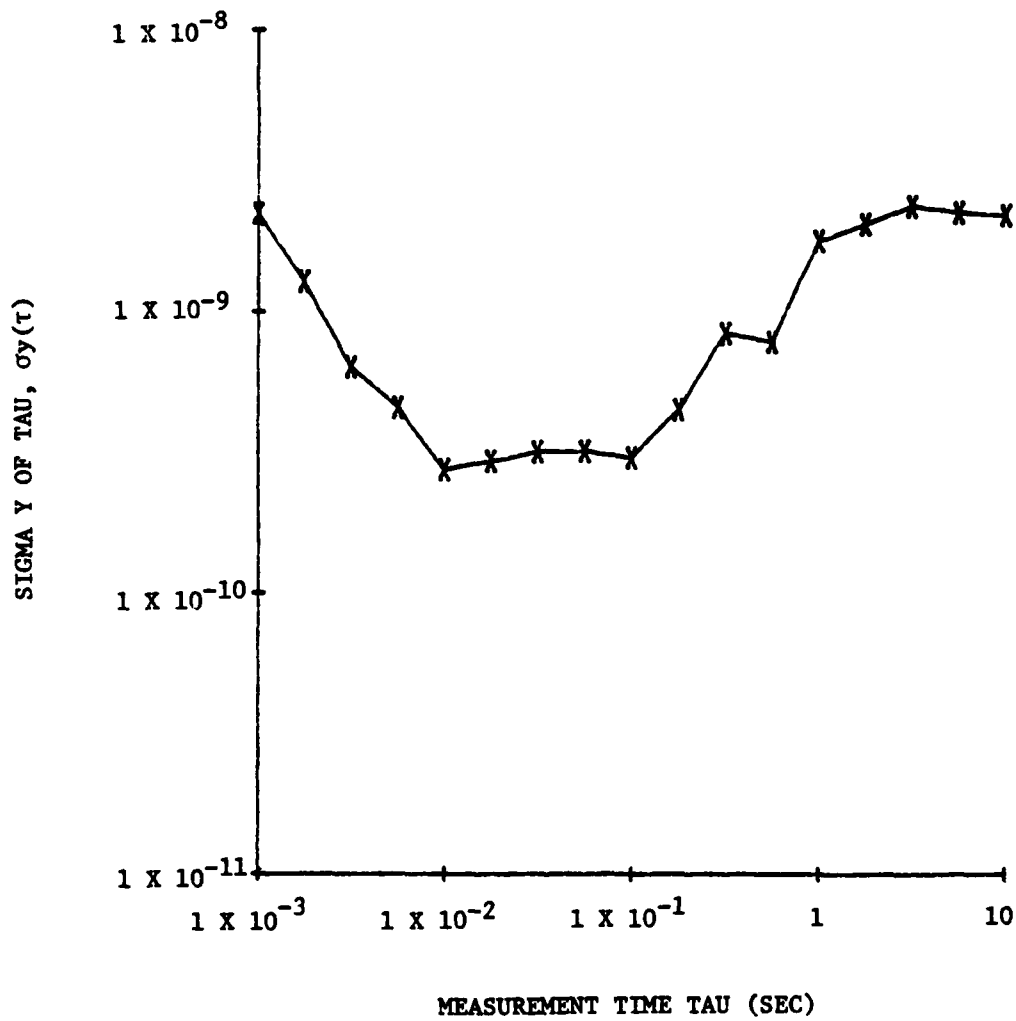oscillator circuits.

Fig. 7 Time domain (Allan variance) stability of SAW oscillators.

the open air. Packaging and sealing the crystal will be necessary to achieve a stability of 1 x 10-11. Frequency domain stability or phase noise was also measured. This is a particularly important parameter for frequency modulated (FM) transmitters and receivers. The single side-band phase noise for the SAW oscillator is shown in Fig. 8. For frequencies offset from the carrier by more than 100 Hz the noise floor will be greater than -100 dB/Hz as shown. This noise floor will be used later when evaluating the signal-to-noise performance of SAW sonobuoy sensors.

3.2   SAW Sensors

An objective of this project was to evaluate the performance of SAW oscillator sensors for potential application to the ASW sonobuoys. Two types of tests were performed: sensing of static and dynamic loads. In the static sensor test the SAW oscillator crystal was loaded about several orientations to determine the basic stress sensitivity. In the dynamic mode test the SAW oscillator crystal was exposed to propagation sound waves in the water tank of a hydrophone calibrator. In this mode the FM modulation or deviation was measure as a function of the sound wave intensity in the water.

3.2.1   Static Pressure Sensors

A test jig to measure the strain sensitivity about any axis of a SAW resonator crystal was fabricated. This was used to obtain information on the frequency deviation vs load characteristics, an anisotropic effect, of SAW resonators. Three types of loading, depicted in Fig. 9 were performed,
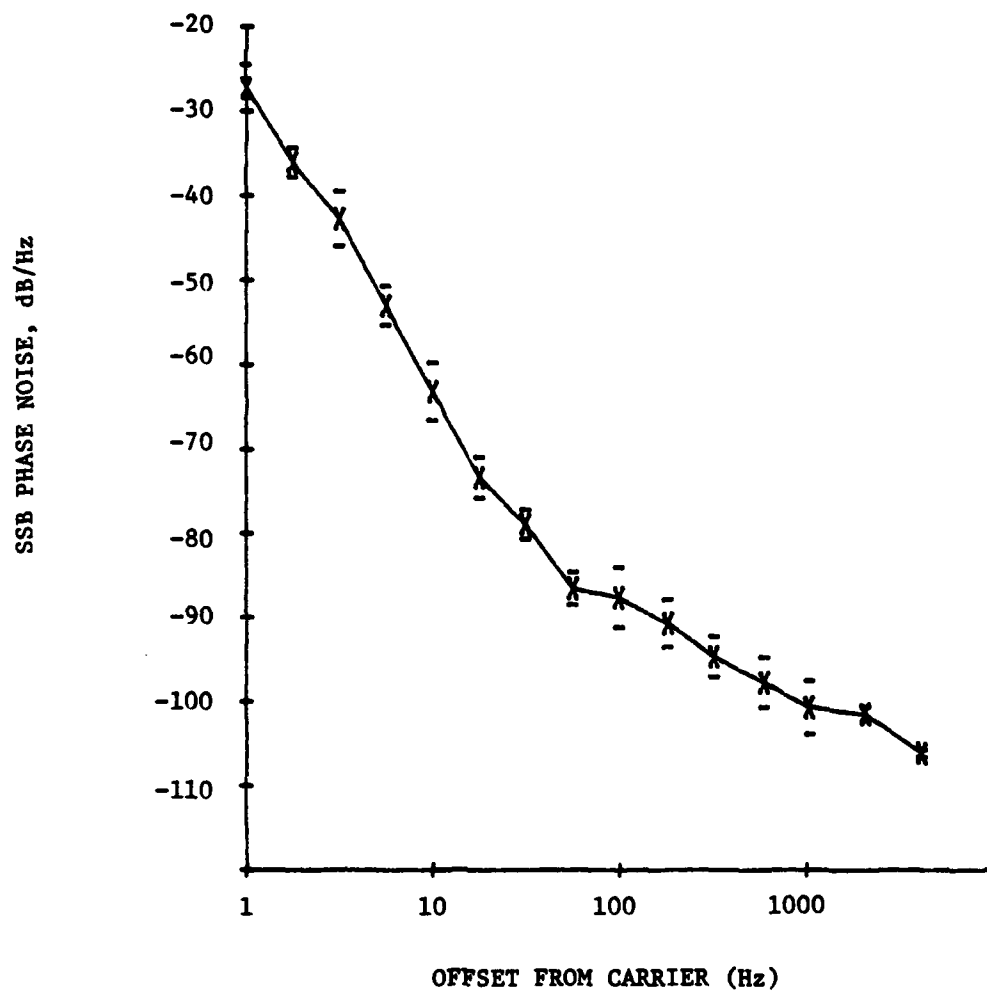
Fig. 8 Frequency domain (single-sideband phase noise) of SAW oscillators.
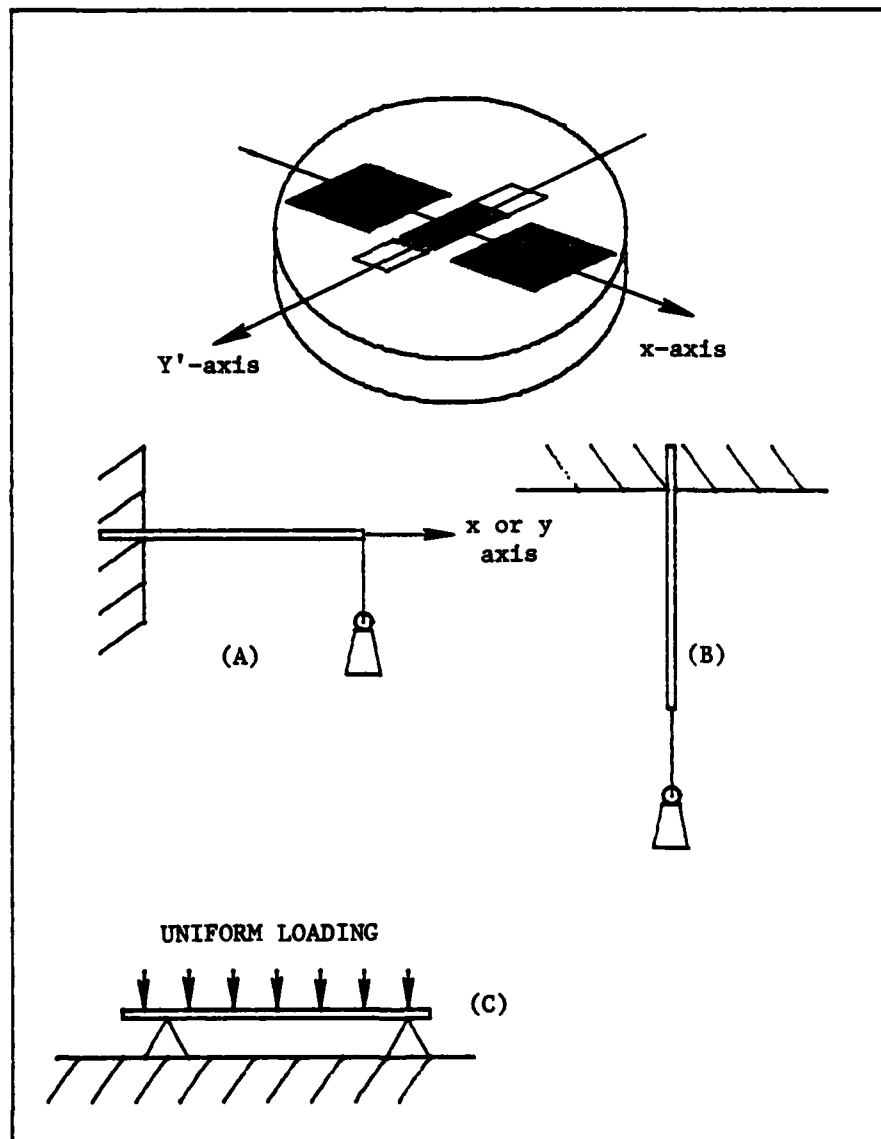
16

Fig. 9 Static loads applied to SAW sensor crystals.
(A) cantilever bending, (B) tension, and
(C) uniformly loaded diaphragm.

17

(a) cantilever bending, (b) simple tension and (c) uniform diaphragm
loading. The results are shown in Figs. 10-14 and summarized in Table II.
The linear coefficients were determined by performing a least squares fit to
the data of Figs. 10-14 and is plotted as a straight line in these figures.
The results of Y'-axis cantilever bending were unexpected and have not been
published to date. Bending (tension) about the Y'-axis of a SAW crystal
produces an upward shift vs a downward frequency shift for X-axis bending.
From this we conclude cantilever-sensor configurations are more sensitive than
diaphragm-sensor arrangements because in a diaphragm the two effects are
present and partially cancelled. This conclusion has prompted us to design
dynamic SAW sensors as cantilever beams.

Table II

Results of Static Loading

Test	Measured Result
1. Catilever, x-axis	-112 Hz/gram
2. X-axis tension	-14.8 Hz/gram
3. Cantilever, Y'-axis	+34.9 Hz/gram
4. Y'-axis tension	+0.3 Hz/gram
5. Pressure Diaphragm	+13.4 Hz/mm Hg
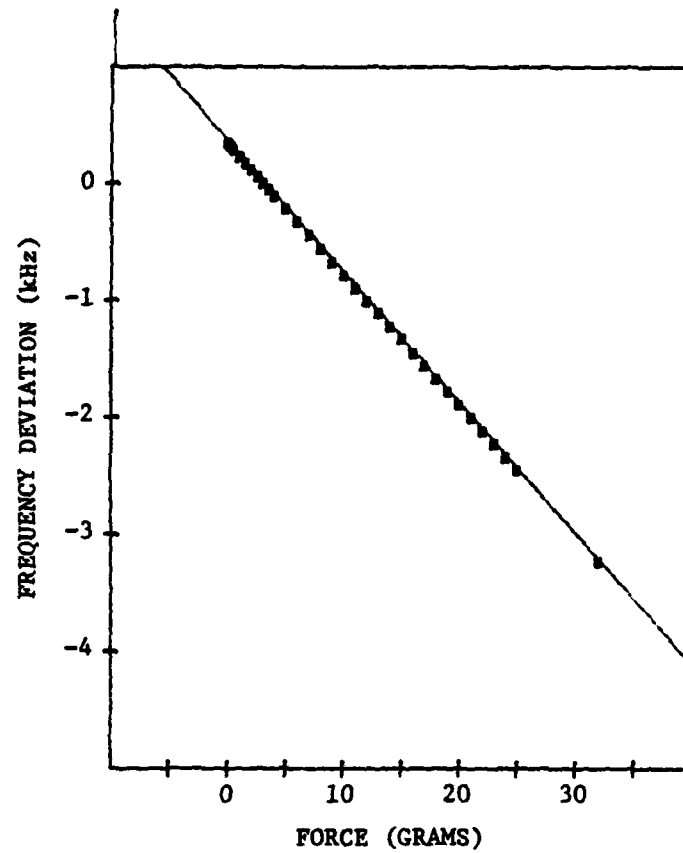
Fig. 10 Cantilever bending in XZ plane.
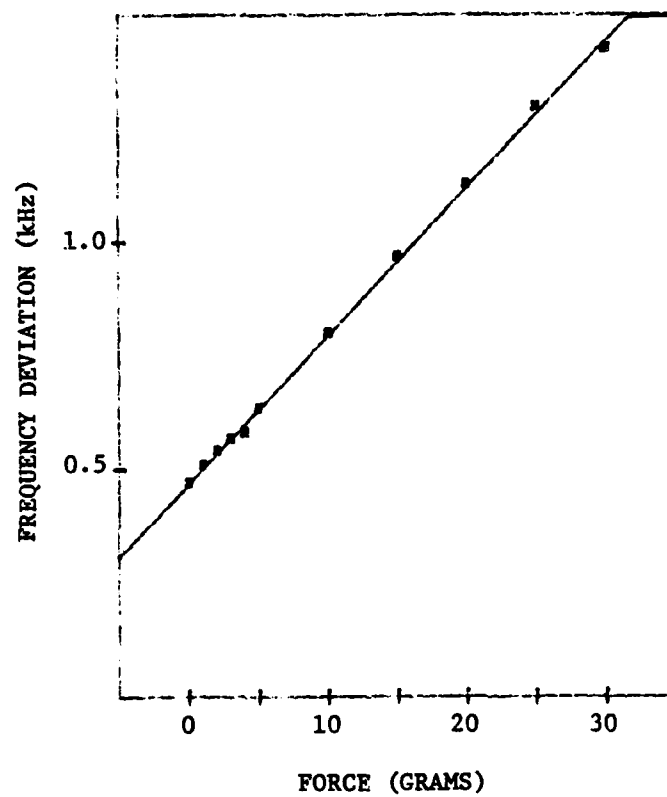
Fig. 11 Cantilever bending in Y'Z plane.

EPC41023.11FR

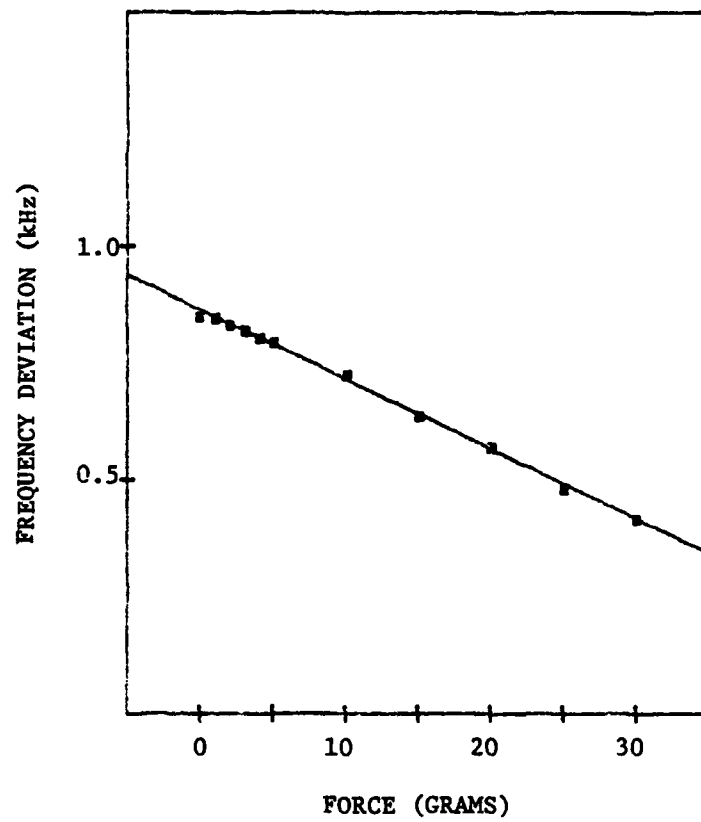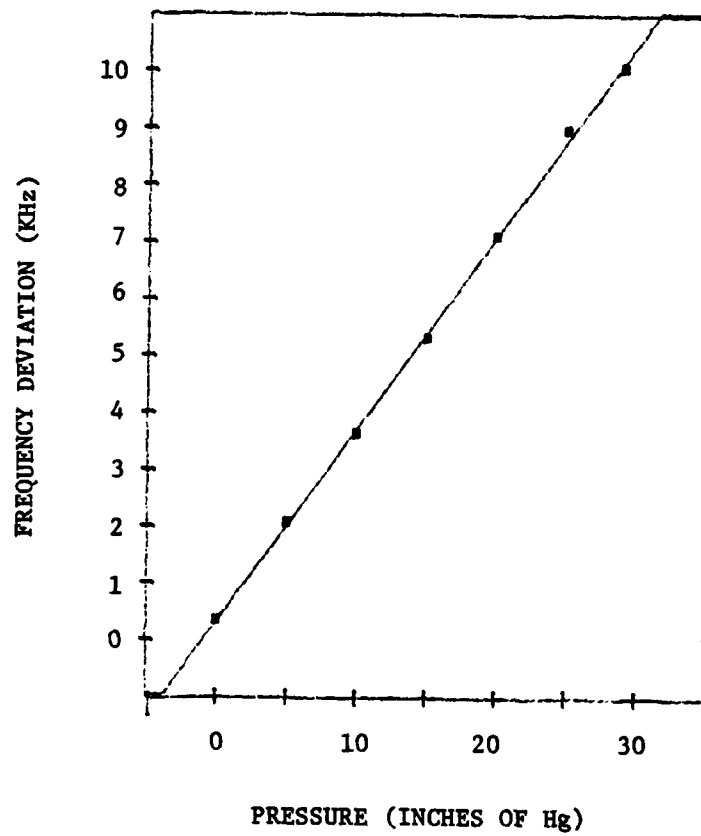Fig. 12 X-axis tension loading.
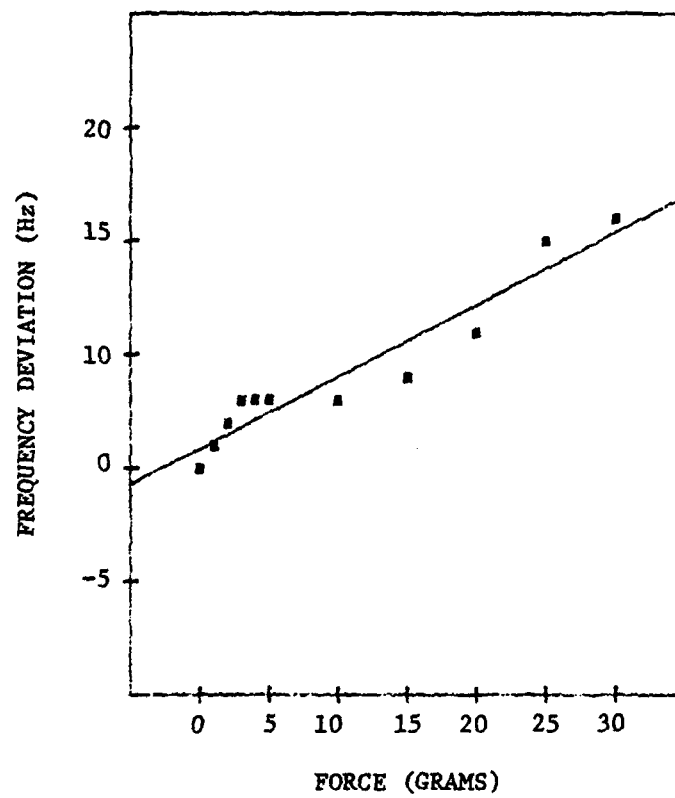
Fig. 13 Y'-axis tension loading.

Fig. 14 Uniformly loaded diaphragm loading.

3.2.2 SAW Hydrophone Sensor

3.2.2.1 Sensitivity

A prototype, cantilever beam, SAW sensor was fabricated using a SAW resonator-oscillator at 61 MHz as shown in Fig. 15. The sensor was placed in a G-19 transducer-water column along with a calibrated (-205.5 dB re 1V/uPa) hydrophone leased from the Naval Research Laboratories in Orlando, Florida. The test set-up is depicted in Fig. 16. In this test set-up the frequency spectrum or sidebands of the SAW oscillator were measured under differing conditions of irradiation by ultrasound in the water column. A photograph of the actual equipment in use is shown in Fig. 17.

Sideband phase noise was measured for different frequencies by holding the intensity fixed at a level of 2 pascal (-80 dBV for calibrated hydrophone). The frequency range covered was 50-1000 Hz. An example of the data taken is shown in Fig. 18a, b and consists of two spectrum plots. Figure 18a is the baseband spectrum of the calibrated hydrophone indicating the presence of a 100 Hz tone with an intensity level of -68.873 dBV (7 pascals). The corresponding SAW hydrophone output spectrum is shown in Fig. 18b. Normally, the measurement system IF was set to 10 kHz and spectrum analysis performed about this frequecny. All of the data over the frequency range 50 to 1000 Hz is contained in Appendix I of this report.
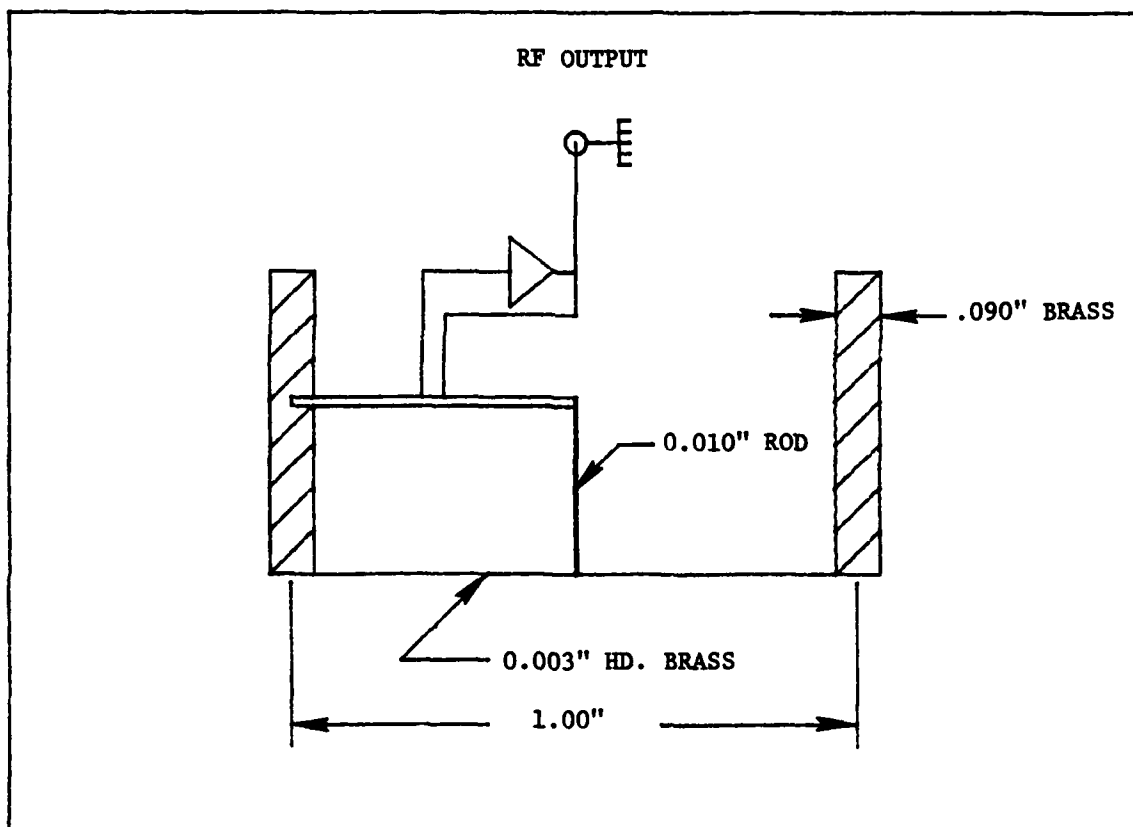
RF OUTPUT

.090" BRASS

0.010" ROD

0.003" HD. BRASS

1.00"

Fig. 15 Prototype, cantilever beam, SAW sensor.

25
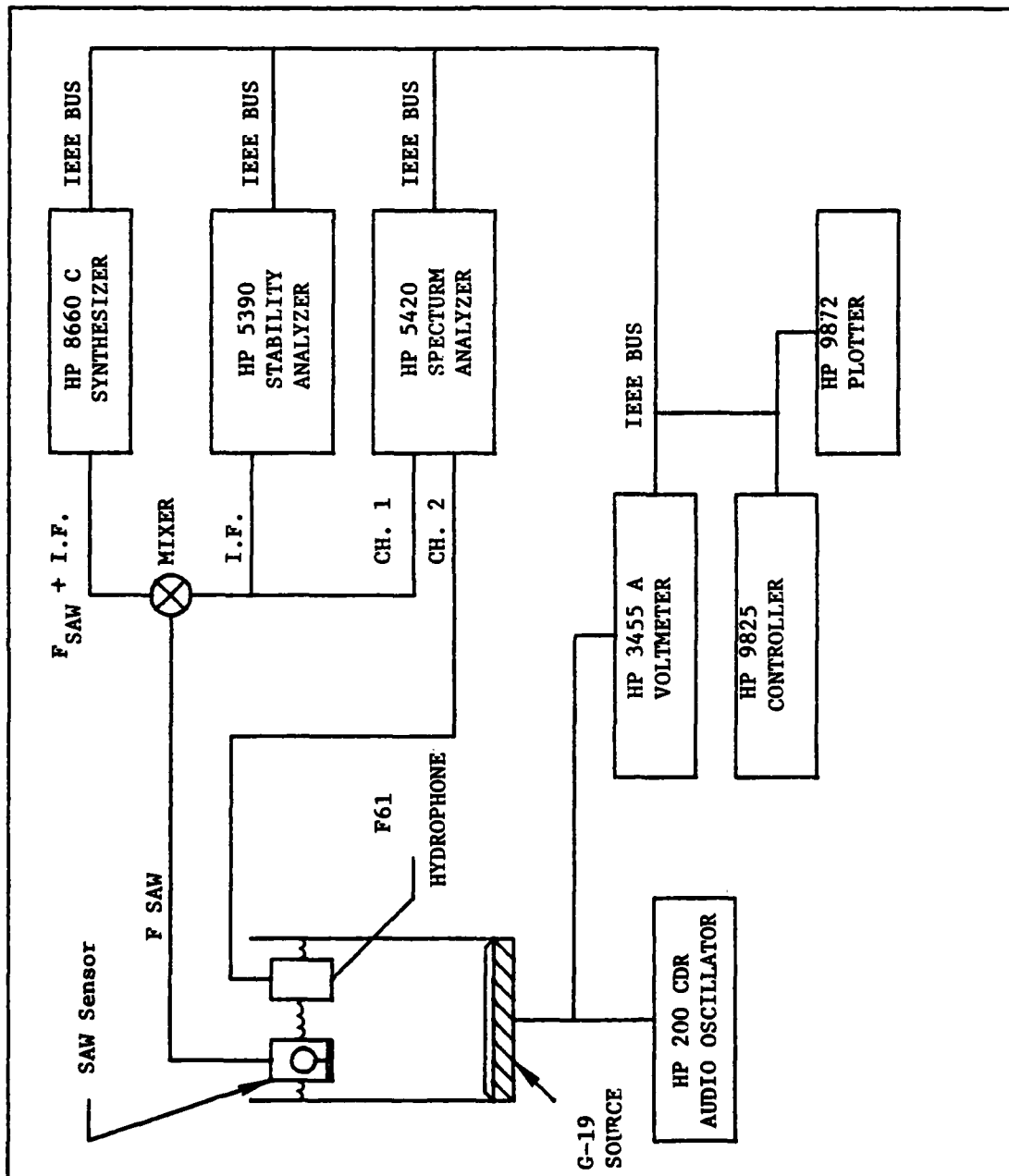
Fig. 16 Experimental testing set-up.

ERC79-5198

Fig. 17   Photograph of measurement set-up.

FRC41023.11FR

X: 9.9329 K   ΔX: 100.26

A SPEC 1   #A: 10   EXPAND

X: 100.00   Y: -68.873

A SPEC 2   #A: 10   EXPAND
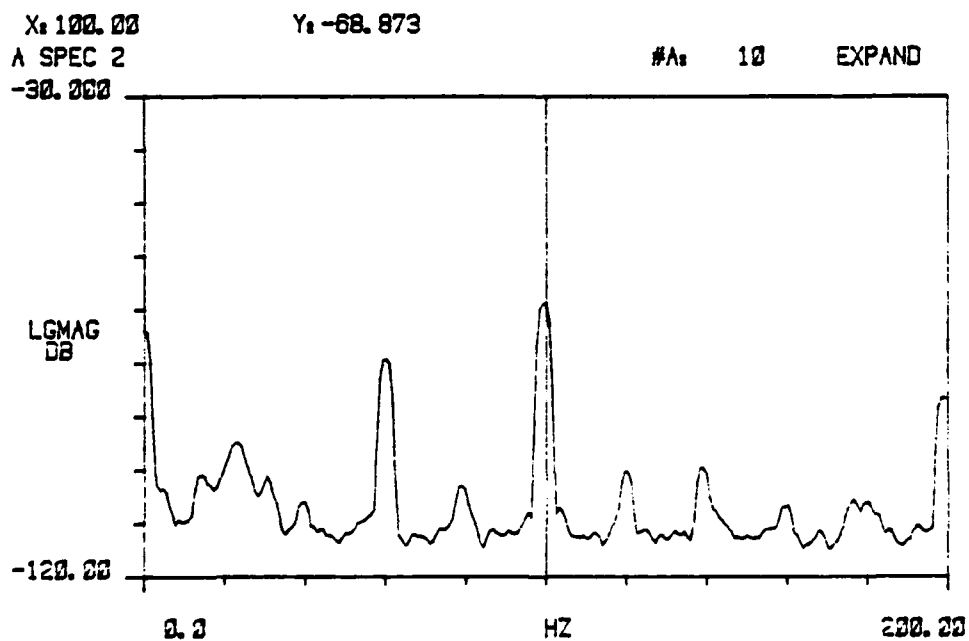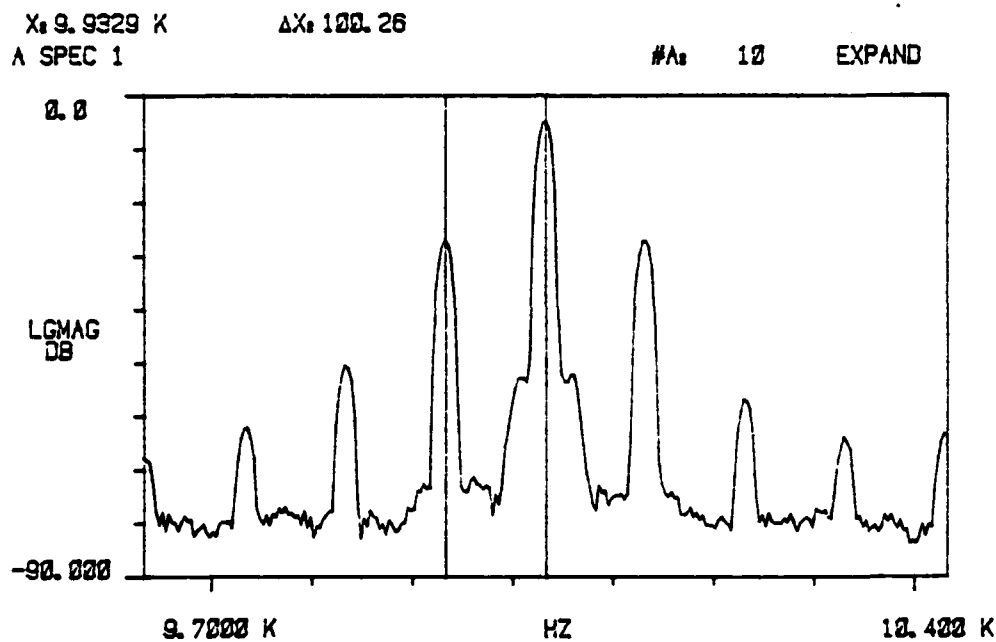

Fig. 18   (a) Baseband hydrophone spectra, and (b) sideband spectra
          of SAW hydrophone.

3.2.2.2 Feasibility Model

A specific task of this project was to fabricate and deliver a
feasibility model surface Acoustic Wave pressure sensor suitable for testing
these devices in existing ASW sonobuoy systems. Shown in Fig. 19 is a
photograph showing several views of the prototype unit. The feasibility
sensor consists of two independent SAW oscillators which are used to generate
an intermediate frequency (IF) output as shown in Fig. 20. The IF for the ASW
sonobuoy system was 125 kHz. One SAW crystal is mounted as a cantilever beam
with one end attached to a sensing diaphram by a rod (not shown in Fig. 19).
Sound waves in the water are transmitted to this crystal resulting in FM
modulation of the IF output. In this system parabolic temperature variations
(Fig. 4) are cancelled to first order. For the feasibility model shown the
temperature coefficient of the IF frequency was 0.049%/°C. The linear change
in IF frequency with temperature is shown in Fig. 21 and is due to the
different thermal expansion coefficients of the mounting arrangements for the
two SAW crystals. Recent results (5) for SAW sensors bonded together with
glass frit so as to minimize this difference, indicate that the temperature
stability of the IF frequency can be reduced to 0.0065%/C. Our experience
with the feasibility model indicates that considerable care will have to be
excercised in matching the thermal expansion coefficients if the IF frequency
is to reamain constant over the required +3 to +30°C operating range.

ERC79-6988
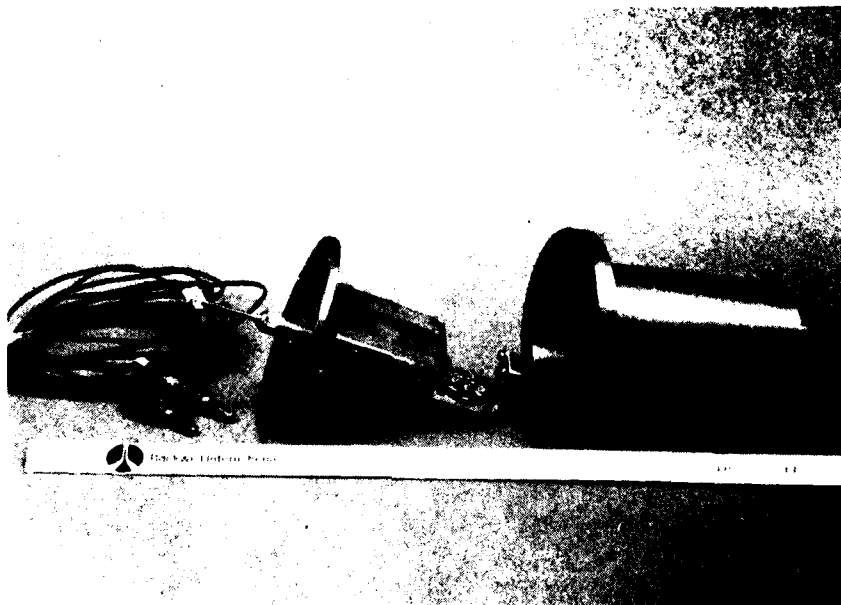

Fig. 19 Feasibility model surface acoustic wave (SAW)
pressure sensor.

ERC41023.11FR

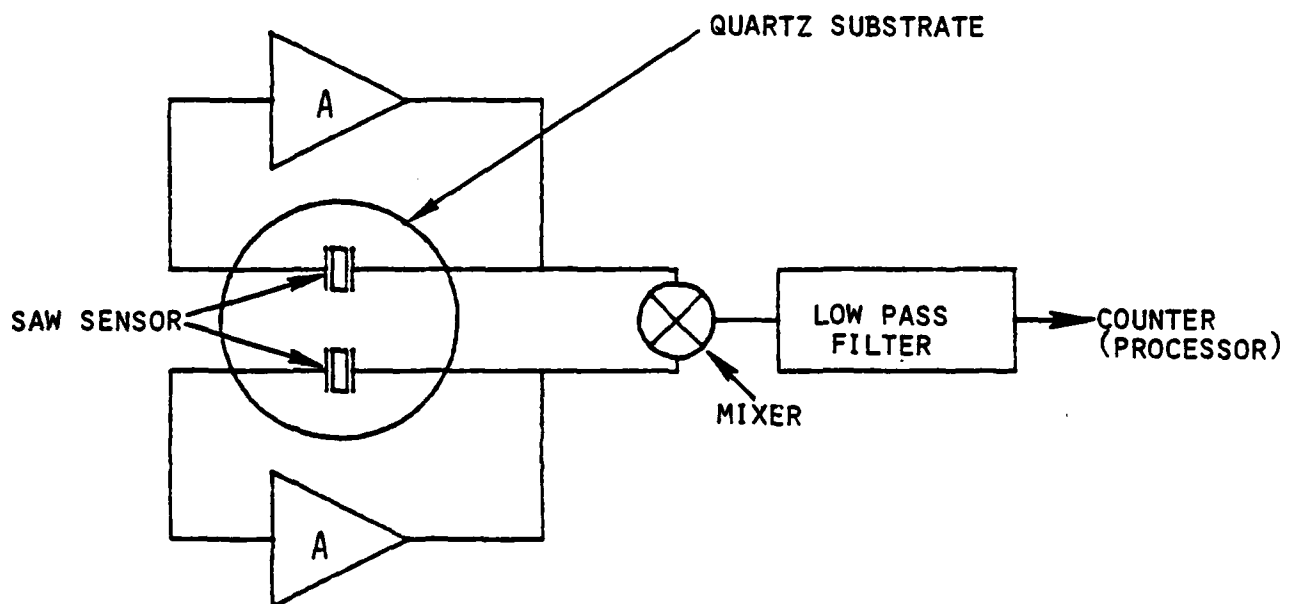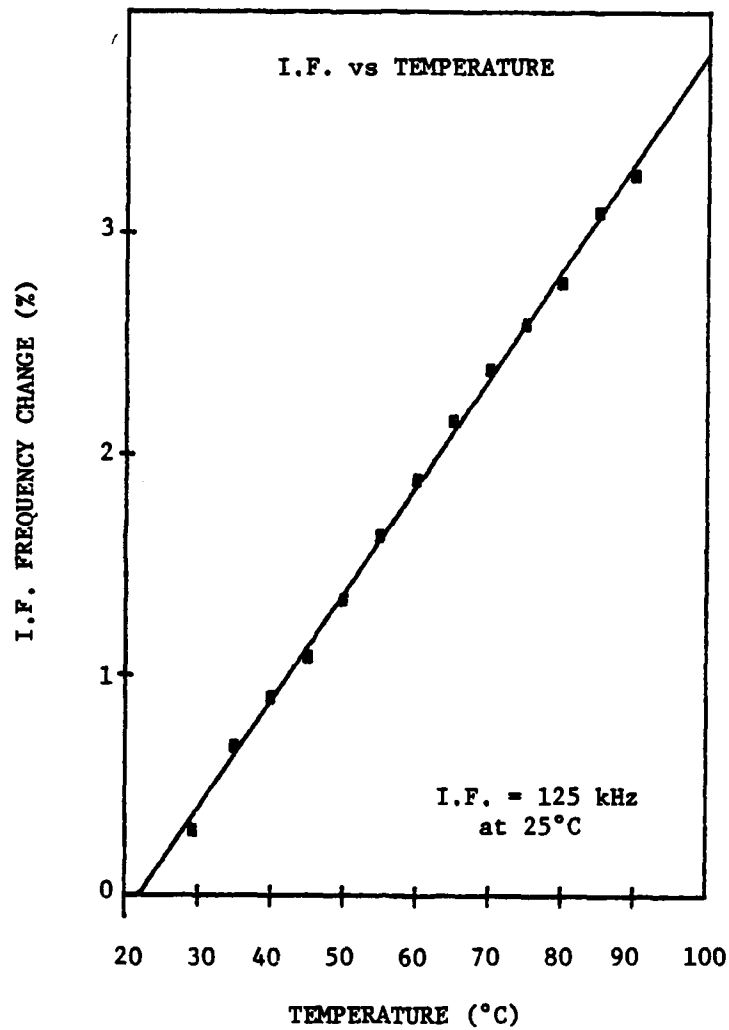Fig. 20 Dual crystal detector for SAW sensor feasibility model.

I.F. vs TEMPERATURE

I.F. FREQUENCY CHANGE (%)

I.F. = 125 kHz
at 25°C

TEMPERATURE (°C)

Fig. 21 IF frequency vs temperature
showing linear characteristic.

3.2.3 Interpretation of Results

Frequency modulation of a SAW oscillator produces an instantaneous frequency which is proportional to the modulating signal at frequency ω_m $(2\pi f_m)$,

$$\omega_i(t) = \omega_c + \Delta\omega \cos \omega_m t$$

where $\Delta\omega$ is the amplitude of the frequency deviation. Since the instantaneous frequency is defined to be the derivative of the phase, the output waveform will be given by

$$e_{FM}(t) = A_c \cos [\omega_c t + \frac{\Delta\omega}{\omega_m} \sin \omega_m t]$$

The peak frequency deviation $\Delta\omega$ is independent of ω_m, while the peak phase deviation $\Delta\theta = \frac{\Delta\omega}{\omega_m}$ is inversely proportional to the modulation frequency. $\Delta\theta$ is commonly referred to as the modulation index.

The amplitude of the FM sidebands can be determined by a Bessel function expansion of the signal waveform,

$$e_{FM}(t) = A_c \sum_{m=-\infty}^{\infty} J_m (\Delta\theta) \cos(\omega_c + m\omega_m)t$$

The amplitude of the first four terms as a function of modulation index is shown in Fig. 22. For the case of the SAW hydrophone sensor the modulation index seldom exceeds 1. The ratio of sideband-to-carrier signal level at each modulating frequency for the data of Appendix II is shown in Table III. The modulation index shown is the amount needed to produce a similar ratio in the Bessel function expansion, i.e., $10 \log[J_1(\Delta\theta)/J_0(\Delta\theta)]$. The frequency deviation is obtained by multiplying the modulation index by the modulating frequency.

Table III

SAW Hydrophone Sideband Levels

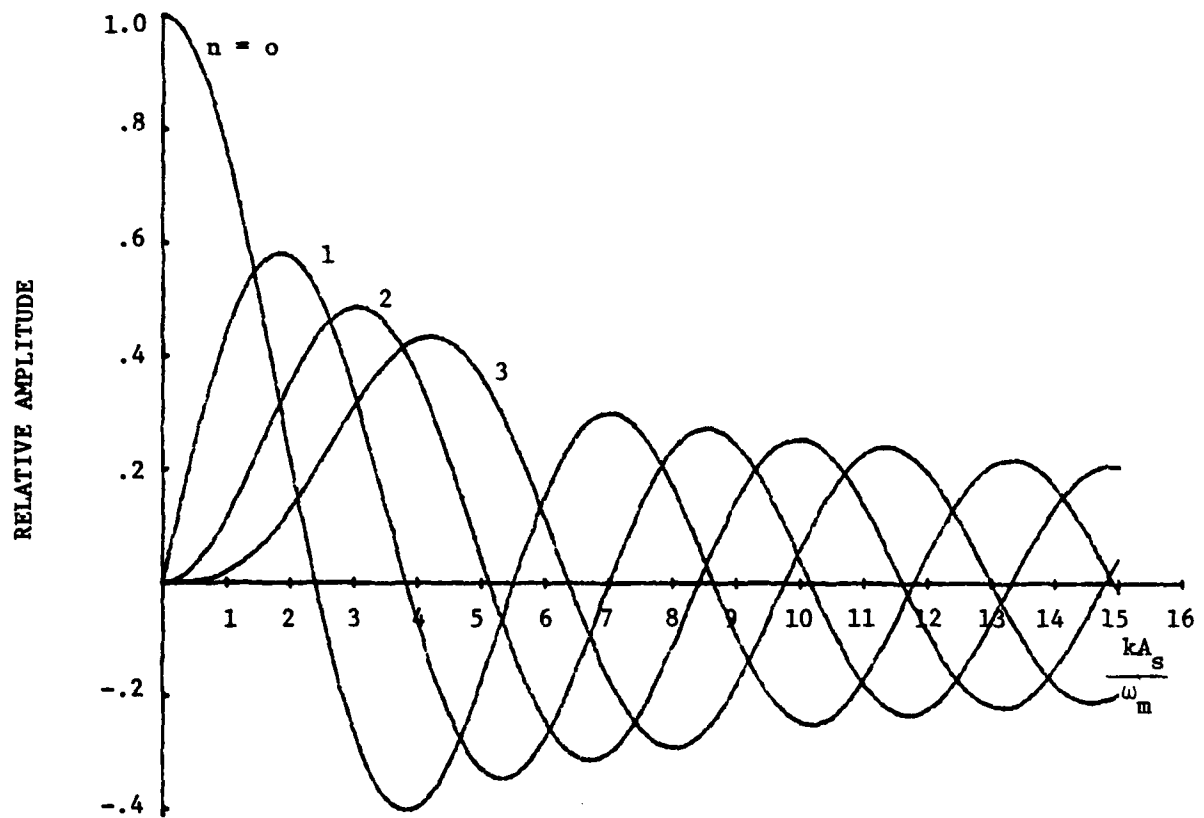| Modulation Frequency (Hz)	Sideband To Carrier (dB)	Modulation Index	Frequency Deviation (Hz)
50	-25.3	0.1089	5.45
100	-39.0	0.0224	2.24
200	-46.0	0.0100	2.00
300	-44.0	0.0125	3.75
400	-45.0	0.0112	4.48
500	-37.5	0.267	13.35
600	-41.1	0.0175	10.50
700	-50.3	0.0061	4.27
800	-58.2	0.0025	2.00
900	-61.1	0.00175	1.57
1000	-63.8	0.00129	1.29

Fig. 22 Bessel function amplitude as a function of argument.

Table IV

Signal-to-Noise of Hydrophones

Frequency (Hz)	S/N Calibrated Hydrophone	S/N SAW Hydrophone
50	35	60
100	35	47
200	35	44
300	35	50
400	35	50
500	35	59
600	35	57
700	35	48
800	35	40
900	35	38
1000	35	36

The ratio of sideband-to-carrier versus modulating frequency with deviation as a parameter is shown in Fig. 23 as well as the values from Table III. A plot of experimental frequency deviation versus modulating frequency is shown in Fig. 24. A peak in the deviation occurs at 500 Hz and is believed due to mechanical resonances in the diaphragm-post linkage of the sensor mounting structure.

The observed FM frequency devation is consistent with the device geometry (Fig. 15) and the results of static cantilever beam loading of the SAW substrate (Table II). A pressure of 1 pascal acting on a surface area of 5.067 cm(1 inch diameter diaphragm) produces a pressure of 0.05168 grams
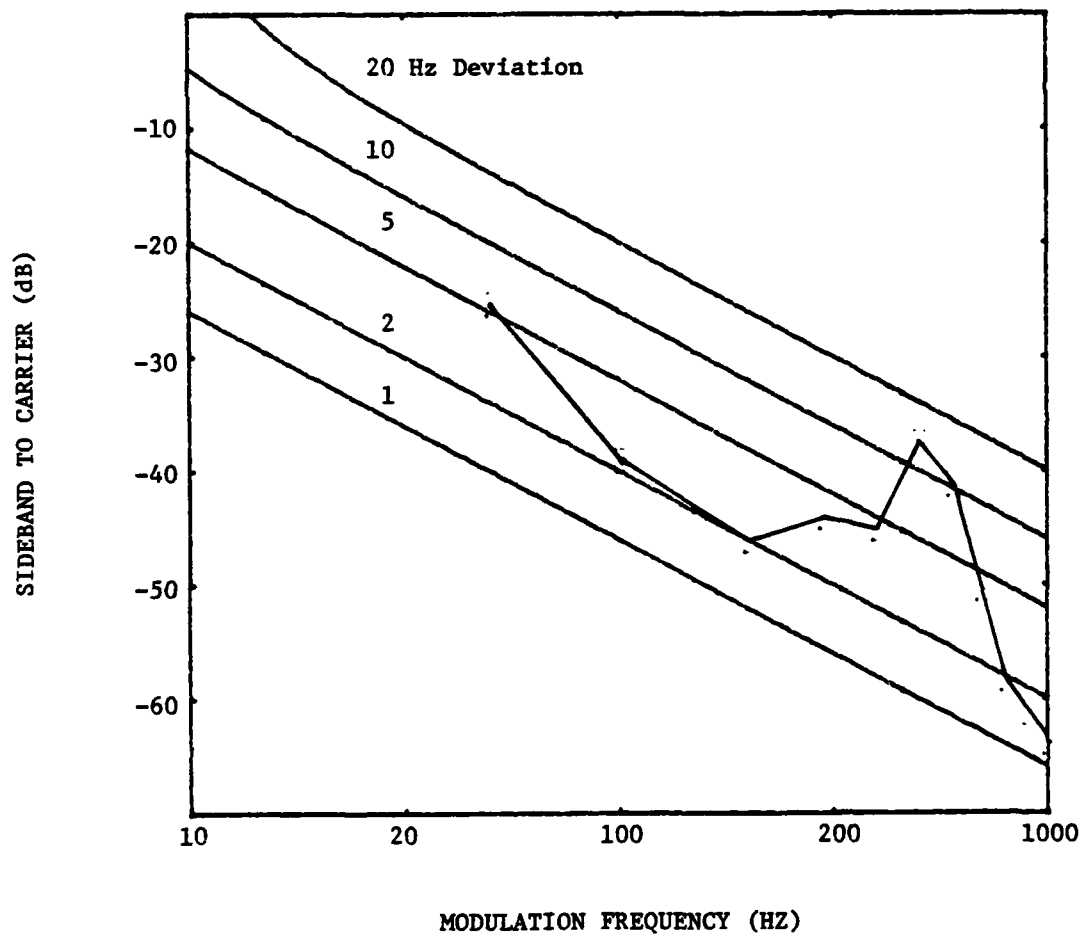
ERC41023.11FP

MODULATION FREQUENCY (HZ)

Fig. 23 Sideband level as a function of modulation frequency.

37

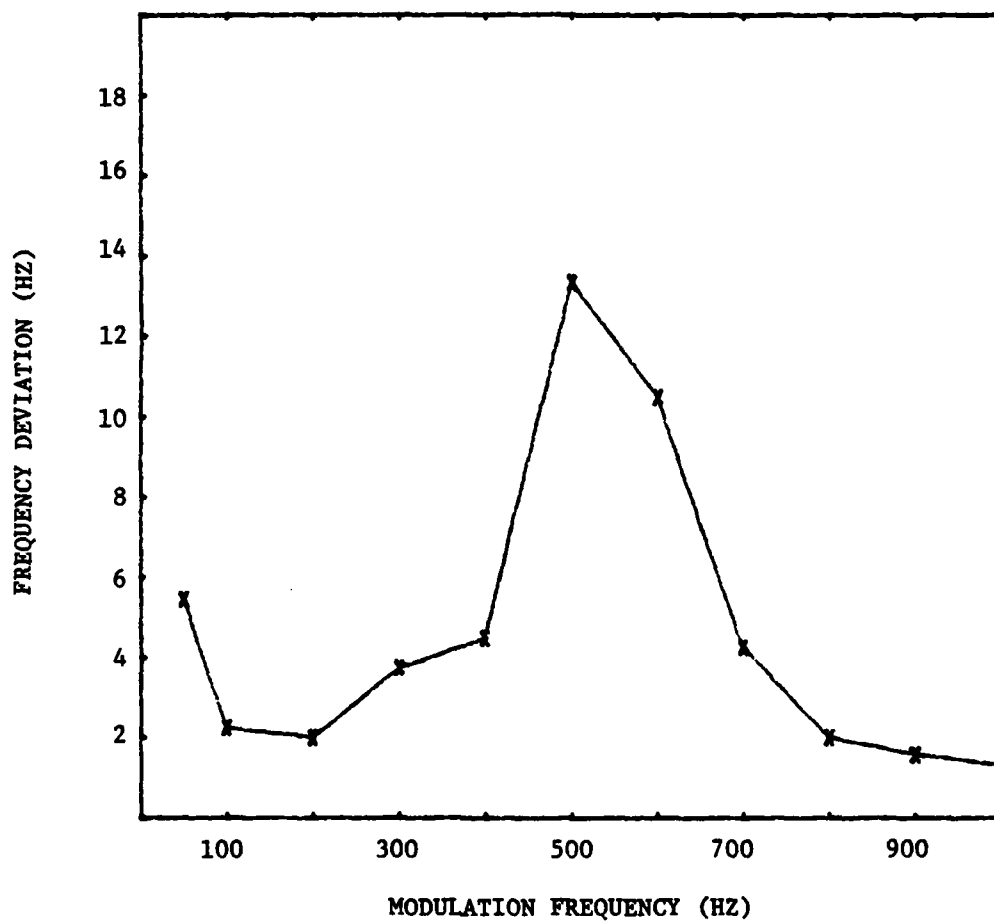Fig. 24 Frequency deviation as a function of modulation frequency.

neglecting any losses in force transmission. From Table II the frequency
constant is -112 Hz/gram, therefore the frequency deviation should be
approximately 6 Hz and is consistent with the experimental results.

From the data contained in Appendix I and the noise floor of the SAW
oscillator, Fig. 8, the signal-to-noise of the SAW sensor can be compared to
the calibrated hydrophone used in the experiments. Signal-to-noise (S/N) for
both is tabulated in Table IV. The calibrated phone had a S/N ratio of
approximately 35 dB over the frequency range tested. The SAW hydrophone S/N
reached a high of 60 dB for low modulation frequencies and became equal to
that of the calibrated phone at approximately 1000 Hz. The apparent increase
in S/N at 500 Hz was due to a mounting resonance discussed earlier. At low
modulation frequencies (<500 Hz) the SAW hydrophone is estimated to be
comparable to a hydrophone with a sensitivity of -180 dB re 1 V/uPa. In the
range <100 Hz the SAW sensitivity improves and is comparable to a -170 dB
phone. The high sensitivity is a result of low phase noise in the SAW
oscillator and increased modulation index at low modulation frequencies.
These results were recently presented[4] at the 1979 ultrasonics symposium.

4.0 CONCLUSIONS

The objective of this project was to evaluate the performance of surface acoustic wave (SAW) oscillators and sensors for potential application to ASW sonobuoys. SAW resonator crystals were fabricated and 12 prototype SAW oscillators characterized. The SAW oscillators were evaluated as stable oscillators as well as frequency modulated (FM) static and dynamic stress/strain sensors.

SAW resonator crystals were designed, photomasks constructed, and prototype oscillators operating at 61 and 61.125 MHz fabricated. Because of the inherent high Q with SAW resonators, very stable crystal controlled oscillators operating on fundamental modes of the crystal over the VHF-UHF range (30-400 MHz) were demonstrated. From the results of our evaluation it is clear that a frequency stability approaching 1×10^{-10} at a constant temperature can be achieved without using sealed crystal enclosures. To achieve stabilities of 1×10^{-11} will require crystal enclosures and better circuit controls including temperature compensation, than are presently used in a single stage oscillator designs.

The results of static loading of SAW resonator crystals indicates that mounting of the SAW sensor as a cantilever beam is preferred over diaphragm type mounting. From the results a sensitivity of -300 Hz/gram of force in a sensor intercepting less than 1 square inch is feasible. SAW sensors which could distinguish forces as small as 0.001 gram were demonstrated.

A SAW oscillator-sensor was configured as a hydrophone and compared in a water tank with a calibrated naval hydrophone. The SAW sensor was found to be at least an order of magnitude more sensitive at frequencies less than 500 Hz. At 1000 Hz the sensitivity of the two types of hydrophone were comparable. The frequency deviation in a SAW is constant and this causes an increase in the signal to noise ratio as the modulation frequency decreases. We conclude that for acousitc detection where the frequencies of interest are in the lower audio range, the SAW sensor is well suited.

In current single channel sonobuoys, a crystal oscillator is operated at one-eighth of the desired RF output frequency. This oscillator's frequency is modified by the action of a voltage-variable capacitor (varactor) to produce an FM modulation on the output frequency which is proportional to the voltage applied to the varactor. This voltage was derived from the acoustic information incident to the hydrophone. Thus, the desired intelligence must undergo two transformations (pressure to voltage, voltage to frequency) before it appears in the proper format. Using a "SAW" device operating at one-eighth of the desired RF output frequency, only one transformation is necessary (pressure to frequency). The "SAW" output, with the FM modulation, is transmitted up from the hydrophone to the transmitter where it is simply multiplied and amplified. This technique simplifies the buoy design by eliminating the electronics used for the extra transformation. This can reduce the size and cost of the sonobuoy, since it is projected that production "SAW" prices will approach those of conventional crystals.

The current technique of using a varactor to modify the source oscillator frequency also degrades the stability of the oscillator. A "SAW" resonator produces the desired modulation with little or no degradation to the oscillator's stability. Thus, this approach yields a more accurate carrier frequency for a given modulation.

Current "SAW" pressure sensors have a sensitivity of 9.7×10^{-5} PPM/Pa, for a 25 mil thickness. Because these "SAW" oscillators are crystal controlled, exceptional frequency stability can be achieved and frequency changes of 0.001 PPM can be observed. This corresponds to a sensitivity of -180 dB referenced to 1 volt per micropascal. This is approximately a 14 dB improvement over conventional hydrophones. In addition, since the information undergoes fewer transformations the system induced noise is a minimum. The noise floor of a "SAW" modulated multichannel sonobuoy would be limited by the phase noise of the synthesizer. Thus, a "SAW" hydrophone would yield a more sensitive sonobuoy system.

Since the current technique transfers the modulation signal from the hydrophone to the transmitter in the baseband, certain problems exist with maintaining amplitude flatness and phase linearity over the information bandwidth. This problem is greatly relaxed by using a "SAW" device since the information is transferred as modulation on a carrier and the information bandwidth is a small percentage of the carrier frequency. In addition, the extension of the information bandwidth toward DC using the conventional approach, necessitates the use of extremely large capacitors which increase the size and cost of the buoy electronics. A "SAW" device has a usable output

down to DC, and since these low frequencies appear only as modulation on a carrier, no extraordinary design measures need be taken. The results of this study have shown the major source of non-linearity in SAW sensors is due to mechanical resonances in the mounting structures. With improved design these resonances can be moved to frequencies beyond the range under consideration.

The direct modulation technique can also be applied to multichannel sonobuoys. In this case, the "SAW" oscillator output frequency will be used to derive the reference of the RF carrier frequency synthesizer. In both the single and multiple channel transmitters, the RF carrier is a multiple of the "SAW" oscillator output frequency. In the multichannel case, this multiplier can change in value, for diferent channel addresses, to produce various RF carrier frequencies, each with the stability characteristics of the reference frequency. Therefore, all the advantages described for the single channel sonobuoy hold for the multichannel sonobuoy as well.

Therefore, through the use of state-of-the-art techniques, this concept greatly simplifies analog sonobuoy design in a unique way. Direct-modulation yields the following advantages:

1. Simplified design - lower parts count

2. Less volume

3. More accurate RF carrier frequencies

4. Extended response to DC

5. Usable for single - multichannel sonobuoys

6. Higher sensitivity

This concept can be used with any communications link, whose output frequency is FM modulated with pressure input information.

At their present development stage, SAW sensors for ASW sonobuoys are limited by (1) a low modulation index and (2) temperature instabilities. The latter problem can be corrected by proper design of the mounting structures and taking into account the coefficients of thermal expnsion. The former represents a far more serious engineering problem if present sonobuoy receivers are to be used with SAW sensors. Present ASW sonobuoy receivers are designed to detect FM signals with high modulation indices. SAW sensor modulation indices are quite low, typically 0.5 or less. Sensitivity is achieved through the low noise characteristics of the sensor rather than by multiplication of a very weak signal. Although the signal-to-noise of a SAW sensor derived signal would be adequate, it could not easily be detected by a conventional sonobuoy receiver because the FM deviation would be small compared to conventional hydrophone outputs to which the receiver is designed. Further research will be needed to either (1) develop a low noise, low modulation index receiver or (2) develop a high modulation index SAW sensor system.

5.0 REFERENCES

1. E.J. Staples, "UHF Surface Acoustic Wave Resonators," 18th Annual Frequency Control Symposium Proceedings, p. 280-285, May 1974.

2. E. Hafner, "The Piezoelectric Crystal-Definitions and Methods of Measurement," Proceedings of the IEEE, V. 57, No. 2, p. 179, 1969.

3. M.E. Frerking, Crystal Oscillator Design and Temperature Compensation, Van Nostrand Reinhold Co., New York, 1978.

4. E.J. Staples, J. Wise, J.S. Schoenwald, and T.C. Lim, "Surface Acoustic Wave Underwater Sound Sensors," to be published in 1979 Ultrasonics Symposium Proceedings, IEEE Cat. # 79CH1482-9SU.

5. D.F. Weirauch, R.J. Schwartz and R.C. Bennett, "SAW Resonator Frit-Bonded Pressure Transducer," to be published in 1979 Ultrasonics Symposium Proceedings, IEEE Cat. #79CH1482-9SU.

6.0 APPENDICES

6.1   Appendix I

Contained in this appendix are 22 spectrum plots arranged as pairs of data into 11 composite figures. Each figure shows the frequency spectrum obtained from the SAW hydrophone and a calibrated hydrophone when exposed to sound waves in water at the frequency indicated. In each figure-pair the lower plot is the spectrum of the calibrated hydrophone at baseband. The frequency of the sound wave is indicated by the cursor and the frequency and voltage level is shown at the top of the plot. The upper spectrum is the SAW sensor spectrum measured either side of the detection IF frequency, typically 10 kHz. The amplitude of the carrier and sideband are marked by cursors and their respective numerical values are printed above the plot.

ERC41023.11FR

X: 1B.B17 K   ΔX: 5B.246   Y: −29.B11   ΔY: 25.293
A SPEC 1   #A: 3

B.B

LGMAG
DB

−9B.BBB

9.7BBB K   HZ   1B.4BB K

X: 5B.BBB   Y: −79.363
A SPEC 2   #A: 2B
−7B.BBB

LGMAG
DB

−12B.BB

B.B   HZ   1BB.BB

Fig. AI-1

47

Fig. AI-2

48

ERC41023.11FR

X: 9.8333 K   ΔX: 200.29   Y: -51.316   ΔY: 45.825
A SPEC 1   #A: 10

X: 200.00   Y: -90.189
A SPEC 2   #A: 10

Fig. AI-3

49

Xₐ 9.7548 K   ΔXₐ 388.89   Yₐ -48.449   ΔYₐ 43.834
A SPEC 1   #Aₐ   18

Xₐ 388.88   Yₐ -88.486
A SPEC 2
                                            #Aₐ   18

Fig. AI-4

50

X: 9.6558 K   ΔX: 399.88   Y: -49.748   ΔY: 44.554
A SPEC 1   #A: 18

X: 488.88   Y: -88.884
A SPEC 2   #A: 18

Fig. AI-5

51

X: 9.5488 K   ΔX: 494.82   Y: -42.849   ΔY: 37.466

Λ SPEC 1   #A: 18

X: 588.88   Y: -88.318

Λ SPEC 2   #A: 18

Fig. AI-6

ERC41023.11FR.

X: 9.4492 K   ΔX: 596.47   Y: -46.258   ΔY: 41.145
A SPEC 1   #A: 18

X: 600.00   Y: -86.475
A SPEC 2   #A: 18

Fig. AI-7

53

ERC41023.11FR

X: 9.3882 K   ΔX: 698.35   Y: -55.104   ΔY: 58.343
A SPEC 1   #A: 18

X: 788.88   Y: -88.926
A SPEC 2   #A: 18

Fig. AI-8

54

FRC41023.11FR

X: 9.2449 K   ΔX: 799.31   Y: -63.571   ΔY: 58.242
A SPEC 1   #A: 18

X: 800.00   Y: -88.881
A SPEC 2   #A: 18

Fig. AI-9

55

X: 9.1634 K   ΔX: 892.39   Y: -68.087   ΔY: 61.136
A SPEC 1

X: 895.25   Y: -98.008
A SPEC 2

Fig. AI-10

ERC41023.11FR

Fig. AI-11